Hindawi
Advances in Civil Engineering
Volume 2019, Article ID 6873096, 12 pages
https://doi.org/10.1155/2019/6873096

Research Article

Seismic Performance Evaluation of a Fully Integral Concrete Bridge with End-Restraining Abutments

Byung H. Choi,[1] **Lorenz B. Moreno**,[1] **Churl-Soo Lim**,[2] **Duy-Duan Nguyen**,[3,4] **and Tae-Hyung Lee**[3]

[1]*Department of Civil Engineering, Hanbat National University, Yuseong-gu, Daejeon 34158, Republic of Korea*
[2]*Sunkoo Engineering Co, Ltd., Sunkoo Square 5th Floor, 85 Anyangpangyo-ro, Uiwang-si, Gyeonggi-do 16004, Republic of Korea*
[3]*Department of Civil Engineering, Konkuk University, 120 Neudong-ro, Gwangjin-gu, Seoul 05029, Republic of Korea*
[4]*Department of Civil Engineering, Vinh University, 182 Le Duan, Vinh 461010, Vietnam*

Correspondence should be addressed to Tae-Hyung Lee; thlee@konkuk.ac.kr

Received 21 September 2018; Revised 2 February 2019; Accepted 26 February 2019; Published 27 March 2019

Academic Editor: Antonio Formisano

A fully integral bridge that is restrained at both ends by the abutments has been proposed to form a monolithic rigid frame structure. Thus, the feasible horizontal force effect due to an earthquake or vehicle braking is mainly prevented by the end-restraining abutments. In a recent study, a fully integral bridge with appropriate end-restraining abutment stiffness was derived for a multispan continuous railroad bridge based on linear elastic behavior. Therefore, this study aims to investigate the nonlinear behavior and seismic capacity of the fully integral bridge and then to assess the appropriate stiffness of the end-restraining abutment to sufficiently resist design earthquake loadings through a rigorous parametric study. The finite element modeling and analyses are performed using OpenSees. In order to obtain the force-deflection curves of the models, nonlinear static pushover analysis is performed. It is confirmed that the fully integral bridge prototype in the study meets the seismic performance criteria specified by Caltrans. The nonlinear static pushover analysis results reveal that, due to the end-restraining effect of the abutment, the lateral displacement of the fully integral bridge is reduced, and the intermediate piers sustain less lateral force and displacement. Then, the sectional member forces are well controlled in the intermediate piers by a proper application of the end-restraining abutments.

1. Introduction

An integral bridge is known as a bridge type that integrates the superstructure and basic substructures. In general, integral bridges are considered as having more economic benefit than a regular bridge because an integral bridge can be constructed without expensive supplemental devices such as expansion joints and bridge bearings [1–8]. Integral abutment bridges (IABs) are commonly used in modern bridge construction, with well over 9,000 IABs in service across the US. Additionally, the integral abutment bridge can be selected as a seismic retrofitting method for existing bridges [9, 10] in addition to the conventional retrofitting techniques [11–13]. In spite of its increasing usage, standard design methods for integral bridges have not been fully established yet that led to the necessity of further research [14–16]. The research study of Far et al. [17] has presented that thermal and seismic loads greatly affect the design of integral abutment bridges due to the integrity of the structure and complex soil-structure-pile interactions. Similarly, there have been studies concerning the seismic behavior of non-IABs [14, 18]. These studies looked into the effects that elastomeric bearings have on energy dissipation, as well as how non-IABs behave as a whole system when subjected to seismic excitation. The studies generally concluded that the bearings, abutment backwall, and pier columns provide a large contribution to an entire bridge's seismic behavior. Kozak et al. [14] have evaluated an existing

integral abutment bridge seismic behavior including all important limit states that could occur in each bridge components. Erhan et al. [19] have demonstrated that integral bridges have superior seismic performance in terms of smaller inelastic structure displacement, rotations, or forces compared to conventional bridges. Additional studies have also considered the individual behavior of the pile-pile cap connection under seismic load and of the girder-abutment connection, both of which are of concern due to the large moments transferred at these locations. Most prior studies concerning the seismic behavior of IABs have not considered the behavior of bridges as a whole, instead focusing on individual components, which may neglect some important interactions between components [14]. Understanding the seismic behavior of bridges is important not only to develop cost-effective designs but also to properly assess existing bridges and their safety immediately after an earthquake. Since there is little experimental data on the seismic response of fully integral bridges, numerical models are essential for understanding structural behavior and ensuring safety in design provisions.

Recently, an innovative fully integral bridge system that is restrained at both ends has been proposed to form a monolithic rigid frame structure [18, 20]. The lateral loads (e.g., earthquake load and vehicle braking force) are mainly carried by the end-restraining abutments. Due to such restraining effect, the fully integral bridge is greatly committed to substantially reduce the section properties of the substructure components except for the abutments, which consequently improves the bridge system's aesthetics, economic efficiency, and seismic performance [21]. In addition, fully integral bridge system eliminates other costly bridge components such as bridge supports, support inspection facilities, and expansion joints while reduces maintenance life-cycle cost due to frequent repair and replacement of bridge components. Thus, it is a low-cost and high-performance bridge system [14, 20–22].

Recently, Choi et al. [21] have provided insights into the load distribution characteristics of a fully integral bridge through a parametric study based on the response spectrum analysis. Their study has shown that the stiffness of the end-restraining abutment has a significant effect on the behavior of intermediate piers. The results show that as the abutment's stiffness increases, the internal forces (i.e., overturning moment and base shear force) at the piers radically decrease and then converge to a certain level. Finally, a prototype design of a fully integral bridge has been proposed such that lateral forces and displacements of the bridge system are adequately restrained. However, due to the linear elastic assumption and a simplified modeling method used in the study, there is an inevitable limitation lying on the application of the analysis results.

This study aims to investigate the seismic capacity of the fully integral bridge with end-restraining abutments and the variation of the seismic performance along with the sectional stiffness of the abutments considering the nonlinear behavior of the bridges. For doing so, the displacement capacity and the ductility ratio are determined from pushover analyses by referring to the specified performance criteria in Caltrans [23], and the seismic demand is obtained from multimode spectrum analysis based on design specifications [23–25]. The capacity and the demand results are compared to conduct a seismic performance evaluation on the fully integral bridge models. Moreover, a series of parametric numerical analysis has been performed along with the variation of design parameters of the end-restraining abutment. Lastly, the required stiffness for effective end-restraining is examined to accommodate the seismic design requirements. It should be noted that all considerations in this study are in the longitudinal direction only because the effect of end-restraining abutments is expected to enhance the seismic capacity of such bridge in the longitudinal direction. In the transverse direction, the integrated abutment is expected to provide some strength and stiffness to the connected superstructure due to an innate frame action. However, the conventional bridge is usually restrained at abutments in the transverse direction, and in this case, the effect of the integrated abutment to enhance the seismic capacity is not significant.

2. Theoretical Backgrounds

2.1. Force-Displacement Curve and Moment Capacity. The seismic capacity of the entire bridge can be evaluated through global displacement and ductility when the plastic hinge is reached according to Caltrans [23]. This piece of information can be accessed by using the force-displacement curves. In order to obtain the force-displacement curve of a fully integral bridge, nonlinear static pushover analysis is carried out. The following basic steps of pushover analysis are implemented, as follows: (1) the lateral load-deformation behavior of the girder, end-restraining abutment, and intermediate pier sections is determined using moment-curvature (M-Φ) analysis, and the results are used to define the finite element model of a fully integral bridge; (2) the pushover analysis is performed along the longitudinal direction, using an increasing monotonic displacement-controlled lateral load pattern, which gives an approximate representation of the relative inertia forces generated at the location of substantial mass, as it reaches its limit of structural stability [23]. It means that each increment pushes the frame, which is the entire integrated bridge system of the study, until the potential collapse mechanism is achieved; (3) the force-displacement curve diagrams are drawn based on the pushover analysis results, where the total applied loads are obtained from the base shear forces and the maximum displacement at a particular location in the top of the entire bridge system; and (4) the bridge ductility and displacement capacity are extracted from the force-displacement curves by applying equation (2). Moreover, the lateral force capacity, F_u, and the moment capacity, M_u, are corresponding to Δ_C, which is determined at the ultimate state of the bridge system and at the potential collapse of this system after the formation of plastic hinge from the analysis results [23, 26].

2.2. Seismic Performance Criteria. The entire structural system must meet the global displacement criteria and the displacement ductility requirements specified in Caltrans

[23]. The bridge system must satisfy the global displacement criteria due to the design earthquake loading, which is expressed as

$$\Delta_D < \Delta_C, \tag{1}$$

where Δ_C is the entire bridge or the frame displacement capacity when the first ultimate capacity is reached by any plastic hinge in the bridge system and Δ_D is the displacement demand, due to the earthquake load effects, which can be estimated by multimode spectrum analysis.

According to Caltrans [23], all ductile members in a bridge should satisfy the displacement ductility capacity requirements. Hence in this study, the entire bridge frame corresponds to all ductile members, due to its innate fully integral characteristic. The displacement capacity, Δ_C, of the entire frame is attributed to its elastic plastic flexibility. The fully integral bridge shall satisfy the displacement ductility capacity, μ_c, defined as

$$\mu_c = \frac{\Delta_C}{\Delta_y}, \tag{2}$$

where Δ_y is the idealized yield displacement of the entire frame at the formation of a plastic hinge.

Each member, including the entire bridge frame, should have a minimum displacement ductility capacity of $\mu_c \geq 3.0$, to ensure dependable rotational capacity in the plastic hinge regions, regardless of the displacement demand imparted to that member.

2.3. Multimode Spectrum Analysis. To estimate the displacement demand, Δ_D, of the fully integral bridge system, a linear elastic multimode spectrum analysis, utilizing the appropriate response spectrum, should be performed by adopting the methodology specified by Caltrans [23]. In order to capture at least 90% mass participation in the longitudinal direction, the number of degrees of freedom (DOFs) and the number of modes considered in the analysis should be sufficient, which is typically 6 and 30, respectively. Since an earthquake may excite several modes of vibration in a bridge, the elastic response coefficient, C_{sm}, should be found for each relevant mode. In multimode spectrum analysis, the structure is analyzed for several sets of seismic forces, each corresponding to the period and mode shape of one of the modes of vibration, and the results are combined using acceptable methods, such as the complete quadratic combination 3 (CQC3) method. Therefore, based on design specifications such as AASHTO LRFD [24], Caltrans [23], and KDS [25], C_{sm} is expressed as

$$C_{sm} = \frac{S_{D1}}{T_m}, \tag{3}$$

where C_{sm} is strongly related to the design earthquake return period (i.e., 1,000 years) and to the soil conditions and seismic zone at the site, S_{D1} is the horizontal response spectral acceleration coefficient, and T_m is the period of the mth mode vibration of the bridge system. T_m is first obtained and calculated based on equation (4) to determine the design earthquake load, $p_e(x)$, which is applied as a distributed load along the whole length of the entire frame model:

$$T_m = 2\pi\sqrt{\frac{\gamma}{p_o g \alpha}}. \tag{4}$$

The design constants α, β, and γ are defined as follows:

$$\alpha = \int v_s(x)dx,$$
$$\beta = \int w(x)v_s(x)dx, \tag{5}$$
$$\gamma = \int w(x)v_s^2(x)dx.$$

Hence, the design earthquake load, $p_e(x)$, is expressed as

$$p_e(x) = \frac{\beta C_{sm}}{\gamma} w(x)v_s(x), \tag{6}$$

where $w(x)$ is the static load per unit length of the bridge structure and $v_s(x)$ is the static displacement that corresponds to the applied uniformly distributed load, p_o.

3. Model Description

The prototype bridge in this study is a seven-span prestressed concrete girder bridge with a total length of 227.0 m and a deck width of 10.9 m, as shown in Figure 1. The length of the first and the last span is 26.0 m, while the length of each span in between is 35.0 m. The superstructure and substructure components are integrated and rigidly connected together. The substructure is formed with end-restraining abutments symmetrically placed at both ends and six intermediate piers between them. The end-restraining abutments are designed as hollow rectangular reinforced concrete (RC) member, while the intermediate piers are wall type RC solid member. The heights of the end-restraining abutment and intermediate piers are 10.0 m and 15.0 m, respectively. Since it is a railway bridge, it is also designed in accordance with the Korean National Railroad Agency (KNR) [27]. The cross-sectional configurations and dimensions of the girders are shown in Figure 2, while the end-restraining abutment and intermediate pier are illustrated in Figures 3(a) and 3(b), respectively. Furthermore, the girders are reinforced by prestressed tendons, SWPC 7B, which consist of 7 strands of Φ15.2 mm steel wire that are twisted together and have a yield tensile strength of 1,600 MPa, the ultimate tensile strength of 1,900 MPa, modulus of elasticity of 200,000 MPa, and elongation of 3.5%. The abutments and piers are reinforced with 636-Φ25 mm and 240-Φ29 mm longitudinal steel bars, respectively. The foundation of the end-restraining abutment and intermediate piers are pile cap and three Φ1.5 m drilled piles that are arranged in the direction parallel to the bridge transverse direction. The material properties used in each component will be discussed in the latter sections.

4. Nonlinear Analysis Modeling and Approaches

The finite element model of the prototype of the fully integral bridge was set up using OpenSees, a specialized

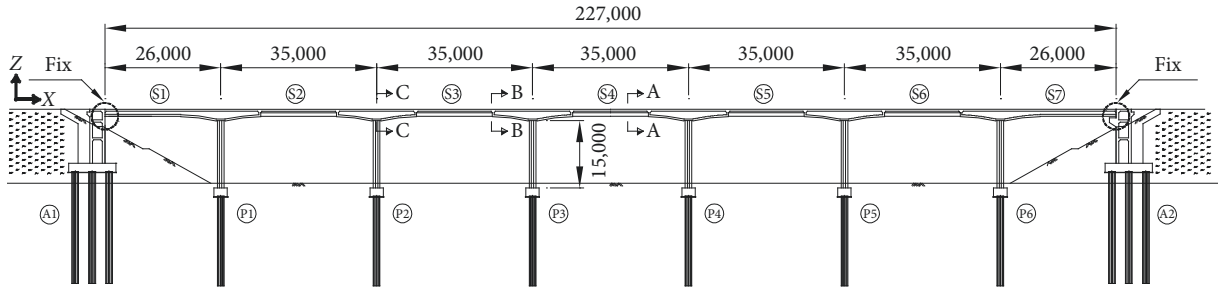

Figure 1: Elevation view of the bridge.

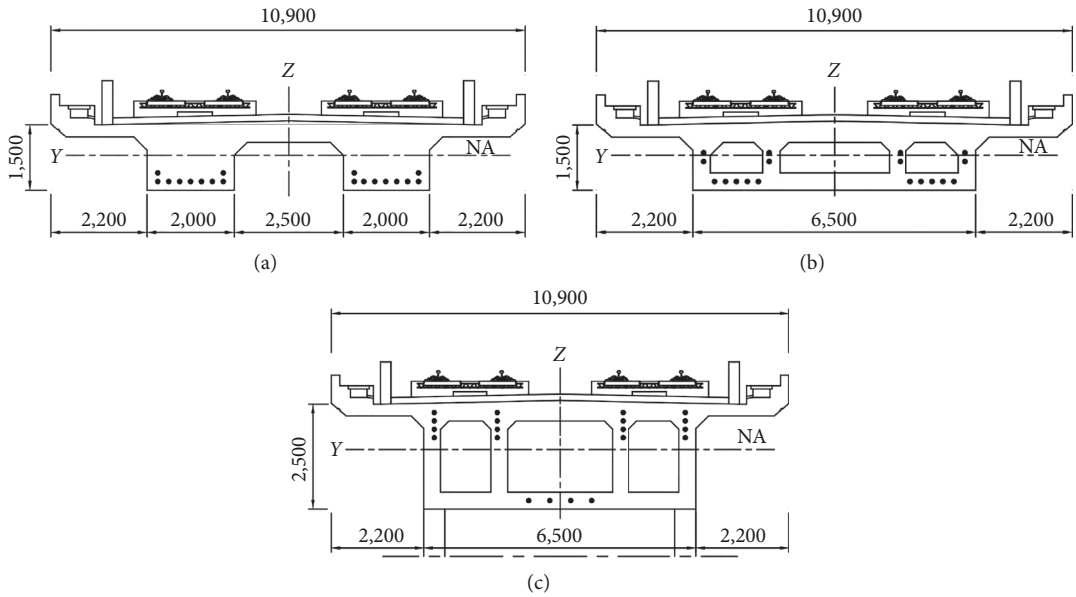

Figure 2: Cross section of the superstructure (unit: mm). (a) Section A-A. (b) Section B-B. (c) Section C-C.

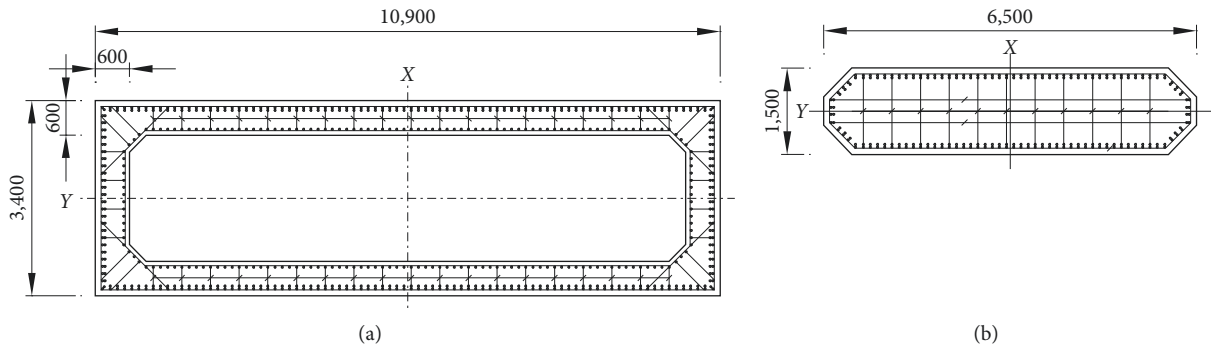

Figure 3: Cross section of the substructure (unit: mm). (a) Abutment. (b) Pier.

structural analysis platform for simulating seismic responses of a structure [28]. To simulate nonlinear inelastic behavior of structural components, fiber modeling scheme is adopted [29]. The end-restraining abutment, intermediate pier, and the part of the girders are expected to behave inelastically at the ultimate state. In the numerical models, the stiffness of the supporting soil is also accounted for where the soil property was considered as soft rock.

4.1. Fiber Element Section Modeling. It was anticipated that bridge girder sections B and C, end-restraining abutment, and intermediate piers will be subjected to inelastic behavior under a severe earthquake loading. In order to achieve an accurate representation of plasticity and nonlinear behavior along the member length, they were appropriately discretized into the finite elements, and then the distributed plasticity model (*dispBeamColumn* element in OpenSees) with the fiber section modeling scheme was used. Figure 4

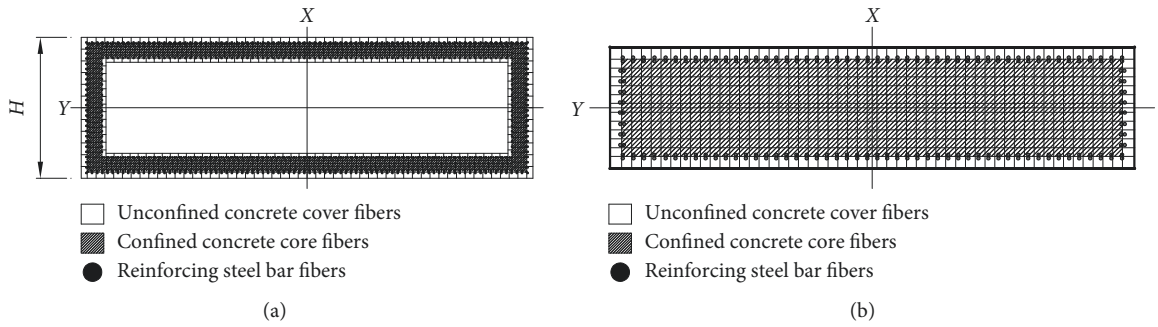

Figure 4: Cross section of the bridge: (a) abutment and (b) pier fiber model.

illustrates the fiber section discretization of the end-restraining abutment and an intermediate pier, which are subdivided into steel, confined, and unconfined concrete fibers. The girder-abutment and girder-pier connections are assumed to be rigid and modeled using rigid links.

4.2. Material Modeling. Since the confinement of concrete by suitable transverse reinforcements increased both the strength and the ductility of compressed concrete [30], the prototype's transverse rectangular hoops and cross ties design and arrangement were considered in the fiber section modeling. In order to rationally reflect such influences, the concrete fibers were further categorized as unconfined (i.e., cover concrete) and confined concrete (i.e., core concrete) [31–33], into which the corresponding material properties were assigned, respectively, as shown in Table 1. An important characteristic of concrete is that it exhibits different behavior in its confined and unconfined states. Apart from higher strength, confined concrete tends to show a much greater ductility when compared to unconfined concrete. Thus, it becomes important and desirable to have a stress-strain model that differentiates the behavior of confined and unconfined concrete. The confined concrete properties were estimated based on the constitutive relationship proposed by Mander et al. [30]. The *concrete02* model in OpenSees, which adopted the Kent-Park model [34] was applied to the concrete of the end-restraining abutments and intermediate piers. This model assumes linear tension softening. The used reinforcing bar material was the SD40 ($F_y = 400$ MPa), which has been commonly used for design and construction of bridge structures in South Korea. In Table 1, f_{pc} is the concrete compressive strength at 28 days, ε_{co} is the concrete strain at the maximum strength, f_{pcu} is the crushing strength, ε_u is the concrete strain at the crushing strength, f_t is the concrete tensile strength, and E_{ts} is the tension-softening stiffness. Figure 5(a) shows the hysteretic stress-strain relationship of the concrete material model.

The longitudinal reinforcing steel bars were added to the cross-sectional modeling as shown in Figure 4. Mechanical properties of the reinforcing bar are listed in Table 2 along with additional parameters defining the stress-strain model adopted in the analysis. The *steel02* model in OpenSees which adopted the Menegotto-Pinto model [35] was used for modeling of the reinforcing bars in the bridge. In Table 2, F_y is the yield strength, E_s is the initial elastic stiffness, b is the strain-hardening ratio, R_0 is a constant between 10 and 20, and C_{R1} and C_{R2} are coefficients defining the shape of the stress-strain diagram. Figure 5(b) shows the hysteretic stress-strain relationship of the steel material model. The moment-curvature relationship of the end-restraining abutment along the longitudinal direction was illustrated in Figure 6.

4.3. Soil-Structure Interaction Modeling. Since it is well known that the soil-structure interaction significantly affects the response of the bridge system under earthquake load [14, 17, 18, 22, 36, 37], the modeling of the piles and its surrounding soil was considered to simulate the soil-pile interaction. As shown in Figure 7, the piles were modeled as linear elastic elements that extend 20 m below the pile cap and the tips of the piles were pinned in place. Figure 7(d) illustrates that on each pile element, a corresponding set of *p-y* and *t-z* nonlinear springs, which used *zerolength* elements in OpenSees, was attached to represent soil foundation. The *p-y* soil spring model [38] in OpenSees represents the lateral resistance of soil foundation. The required ultimate capacity of the soil was determined based on Reese et al. [38] equations and tables. Moreover, the *t-z* soil spring model in OpenSees represents the friction which may act on the piles when they move vertically [18]. The required ultimate shear capacity of the soil was determined based on API [39] suggested equations and values. Concurrently, it is conservatively assumed that the end-restraining abutments should sustain the lateral forces without the supporting effect of the abutment-backfill.

5. Analytical Study Results

5.1. General Observation and Behaviors. In this section, the pushover analysis result of a prototype design is discussed. As shown in Figure 8, the load distribution was applied at the top node of each abutment and piers in the longitudinal direction consistent with the distribution of the masses within the model. The pushover analysis was conducted using the displacement-controlled procedure. The displacement control node was located at the top node of the

Table 1: Concrete material properties.

	f_{pc} (MPa)	ε_{co}	f_{pcu} (MPa)	ε_u	f_t (MPa)	E_{ts} (GPa)	Remarks
Superstructure	40.0	0.002	8.0	0.005	3.27	1.22	Unconfined
	51.5	0.004	25.0	0.024	3.27	0.55	Confined
Substructure	30.0	0.002	6.0	0.005	3.27	1.22	Unconfined
	36.0	0.004	23.1	0.024	3.27	0.55	Confined

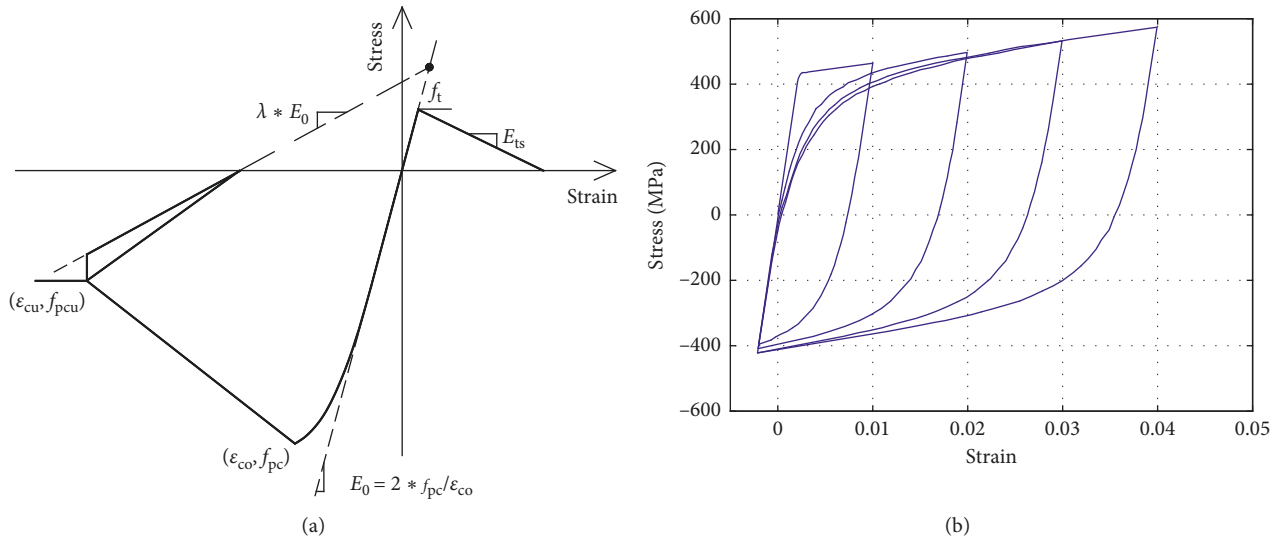

Figure 5: Hysteretic stress-strain behavior of (a) *concrete02* and (b) *steel02*.

Table 2: Reinforcement steel properties.

	F_y (MPa)	E_s (GPa)	B	R_0	C_{R1}	C_{R2}
Steel	400	200	0.01	18	0.925	0.15

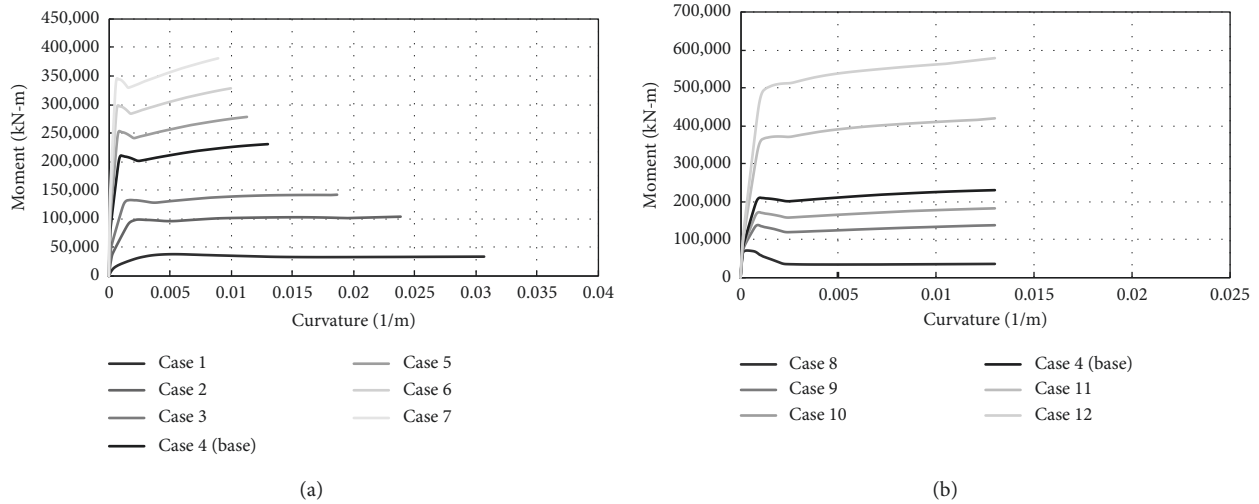

Figure 6: Moment-curvature relationship of the abutment along the longitudinal direction. (a) Variation in sectional area. (b) Variation in reinforcement steel.

left abutment. The deformed shape of the prototype at the final load step of the pushover analysis is shown in Figure 9(a). It should be noted that the deformation of the bridge is exaggerated for a clearer view. Figure 9(b) illustrates the general longitudinal pushover response of the prototype bridge, where it can be observed that the design

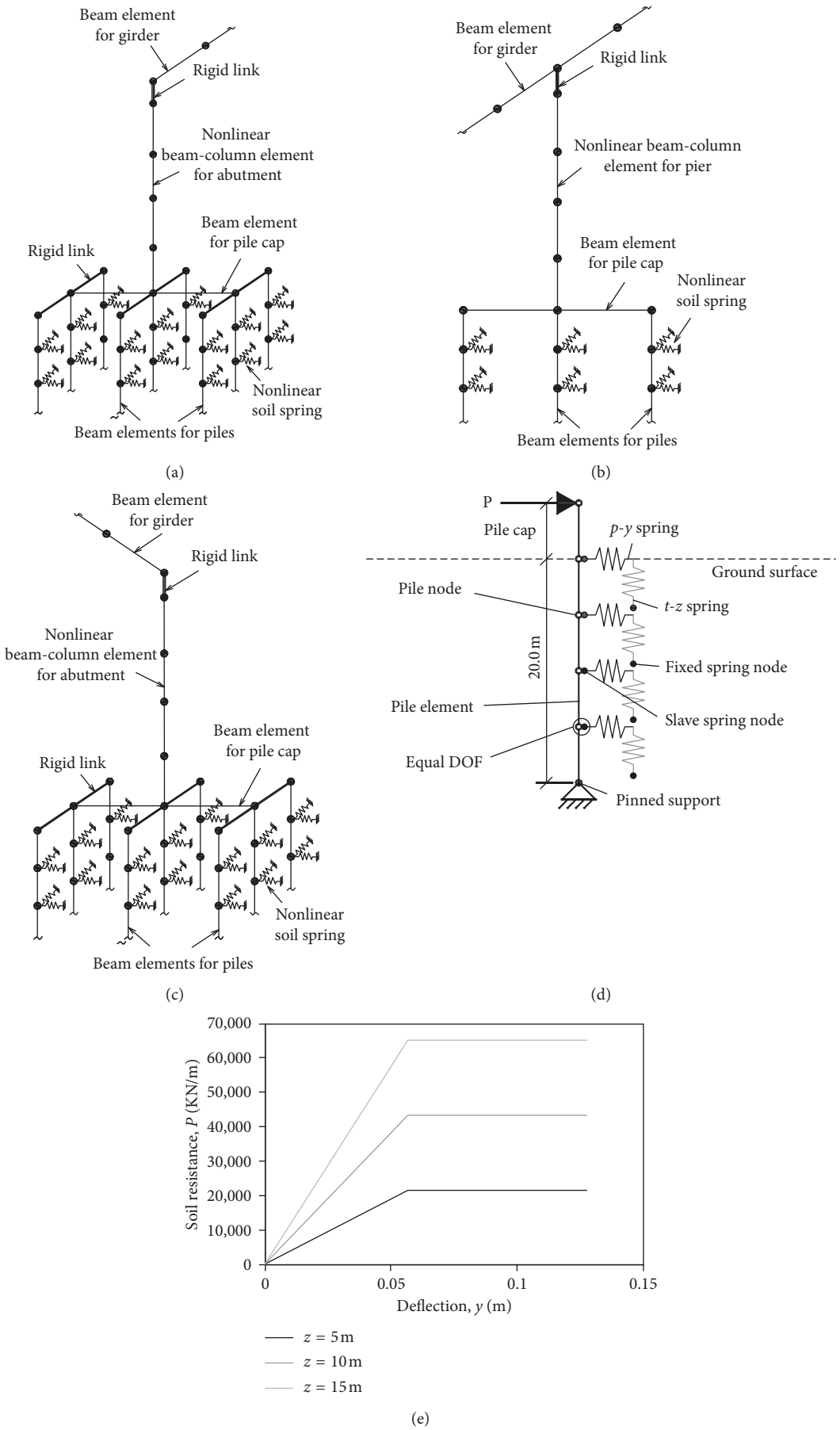

Figure 7: Element discretization of the (a) left abutment, (b) pier, and (c) right abutment pile foundation. (d) Soil-pile interaction. (e) *p-y* curve.

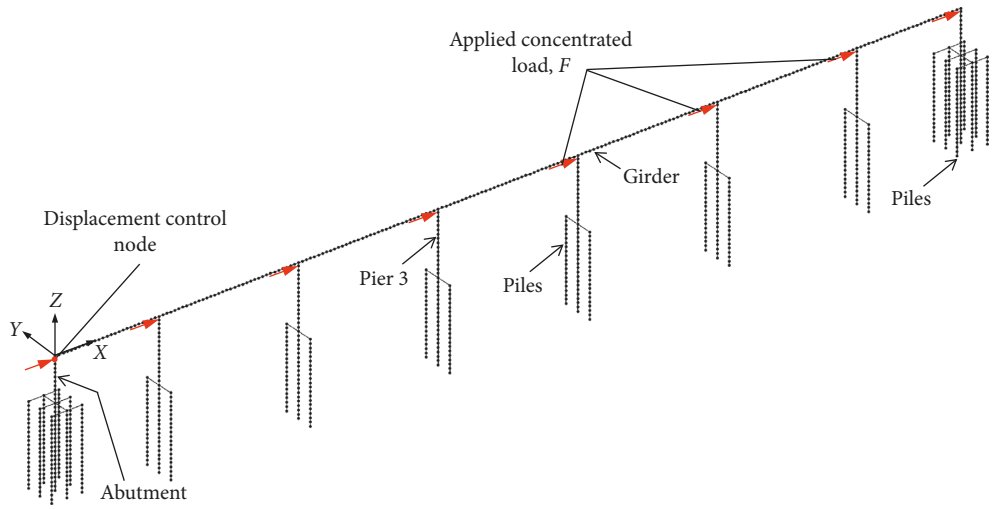

Figure 8: Fully integral bridge model load distribution.

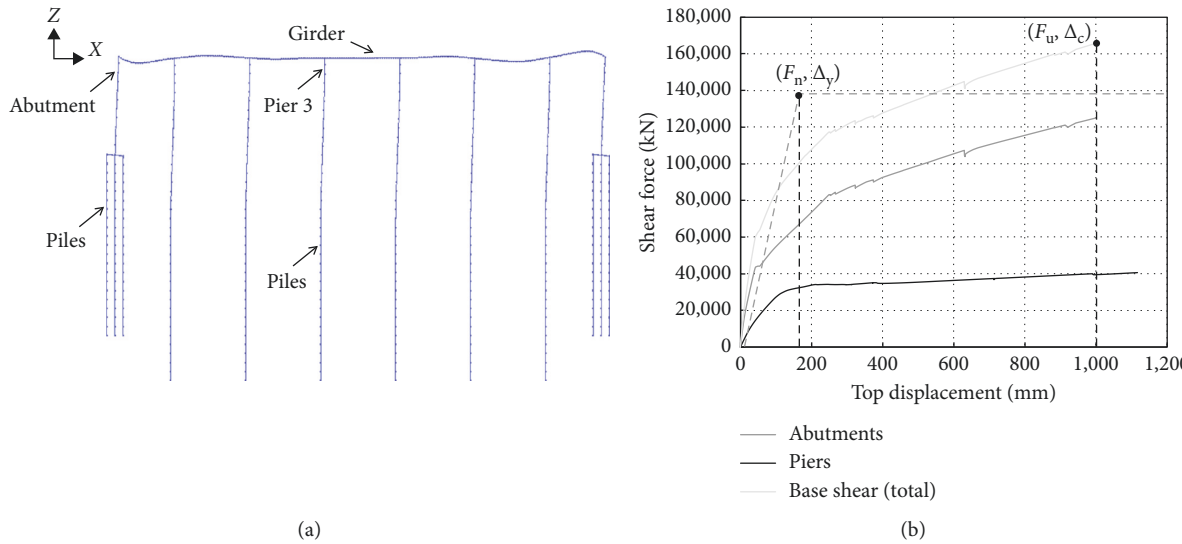

Figure 9: Longitudinal pushover response of the fully integral bridge prototype. (a) Deformed shape. (b) Force-deflection curve.

earthquake load is resisted by the entire frame action of the abutments and piers. Even though the intermediate piers exceed their yielding point, an increasing slope is still observed in the pushover curve of the entire frame. This indicates that the ultimate displacement capacity is dominantly affected by the strength of the end-restraining abutments, and that most of the entire base shear force is sustained by the end-restraining abutment with appropriate stiffness.

5.2. Seismic Performance Evaluation. The seismic performance of the prototype was evaluated with respect to the bridge displacement capacity. Moreover, the displacement capacity of the entire frame and each substructural component was evaluated. Table 3 shows the comparison between the displacement demand and capacity of the prototype bridge. As previously mentioned, the demands of the displacement and the member forces were derived from the multimode spectrum analysis. By comparing the demand and capacity of the prototype model, it is observed that the seismic capacities of the substructure are immensely larger than the nominal seismic demands. The results assert that the fully integral bridge with end-restraining abutments should retain a higher-level seismic capacity compared to the general integral abutment bridges as well as conventional bridges and, thus, it may provide a possible option to an innovative design. It should be noted that the investigated bridge was newly designed for this study according to KNR. It confirms that the current design code does not accommodate the benefit of the end-restraining abutment, and subsequently, some structural members might be overdesigned.

It can also be observed that the displacement ductility capacity of the entire bridge frame, μ_c, is 6.54, which is greater than the minimum capacity ductility criteria

Table 3: Comparison of demand and capacity results.

Member	Displacement (mm)		Base shear force (kN)		Overturning moment (kN-m)	
	Demand	Capacity	Demand	Capacity	Demand	Capacity
Abutment	7.5	1000.0	12,962	125,098	139,549	1,250,977
Pier 3	10.1	1116.1	2,283	40,564	14,524	405,640

Table 4: Parametric analysis results.

Case	Dimensions of abutments				Results	
	H (mm)	A_c (m^2)	A_s (cm^2)	I_y (m^4)	Δ_c (mm)	M_u (kN-m)
1	1500	9.25	5.07	1.7	1,000.0	81,930
2	1900	14.1	5.07	6.8	1,000.0	226,528
3	2400	14.7	5.07	12.8	1,000.0	325,894
4 (base)	3400	15.9	5.07	31.1	1,000.0	554,038
5	3900	16.5	5.07	43.5	741.0	610,207
6	4400	17.1	5.07	58.3	696.5	707,486
7	4900	17.7	5.07	75.	825.5	854,972
8	3400	15.9	0.71	27.8	1,200.0	138,840
9	3400	15.9	2.87	29.3	1,000.0	342,604
10	3400	15.9	3.87	31.0	1,200.0	475,885
11	3400	15.9	9.57	34.3	666.3	818,519
12	3400	15.9	13.4	37.3	448.2	855,041

specified by Caltrans [23] to ensure dependable rotational capacity. In addition, the global displacement criteria were also satisfied, in which the total displacement capacity of the fully integral bridge was 1,000 mm against its nominal displacement demand of 7.5 mm.

5.3. Parametric Study Results. Since integrated abutments play a crucial role in structural behaviors of fully integral bridges, a parametric study was performed with respect to the dimension of the abutment. Meanwhile, the other influential parameters to the seismic behavior of such bridges were fixed to examine the effect of the abutment's properties thoroughly. The parametric pushover analysis results are shown in Table 4, which have been obtained according to the variation of design parameters of the abutment. H is the abutment section thickness as shown in Figure 4(a), A_c is the total concrete area of the abutment, A_s is the area of one reinforcing steel bar, and I_y is the moment of inertia of the abutment section about its weak axis. It should be noted that the base model used in the previous sections is Case 4.

The analysis results reveal that the bending capacity of the fully integral bridges increases proportionally to the abutment stiffness by utilizing a larger section or steel reinforcement. The displacement ductility capacity of each case was found to be greater than 3.0. It means that each case also satisfied the specified minimum capacity ductility criteria by Caltrans [23]. In Figure 10, the overturning moment-lateral displacement curves of the end-restraining abutments demonstrate the nonlinear ductile behavior with respect to the parametric ranges. It is apparent that there is a minimal decrease in the structural ductility as the strength considerably increases. This also verifies the tendency that the end-restraining abutment carries most of the total system base shear force as its bending capacity increases.

Figure 11 represents the variation in the top lateral displacement of the piers along with the horizontally applied loading, F. It can be observed in Figure 11 that the lateral displacement radically drops along the abutment stiffness and converges into a value around Case 4. It means the lateral displacement of the entire bridge could be restrained effectively if the abutments hold a sufficient stiffness. For example, if it is supposed that the lateral displacement must be restrained within 12.0 mm when subjected under an earthquake effect of 20,000 kN, it can be determined from the parametric study results that the required stiffness for the abutments should be the same or larger than that of Case 4.

The sectional moment allocated at the intermediate piers also shows the same tendency of decreasing along with the abutment's bending stiffness as represented in Figure 12. Thus, it seems to be insignificant to further increase the sectional stiffness of the end-restraining abutments beyond the converging point (Case 4).

6. Conclusions

This study investigated the seismic behavior and nominal capacity of the fully integral concrete bridge with an end-restraining abutment. A series of nonlinear static pushover analyses were carried out to evaluate the seismic performance of the fully integral bridge. Based on the analysis results, the following conclusions are drawn:

(1) The ultimate displacement capacity of the fully integral concrete bridge with end-restraining abutments was primarily affected by the stiffness of the

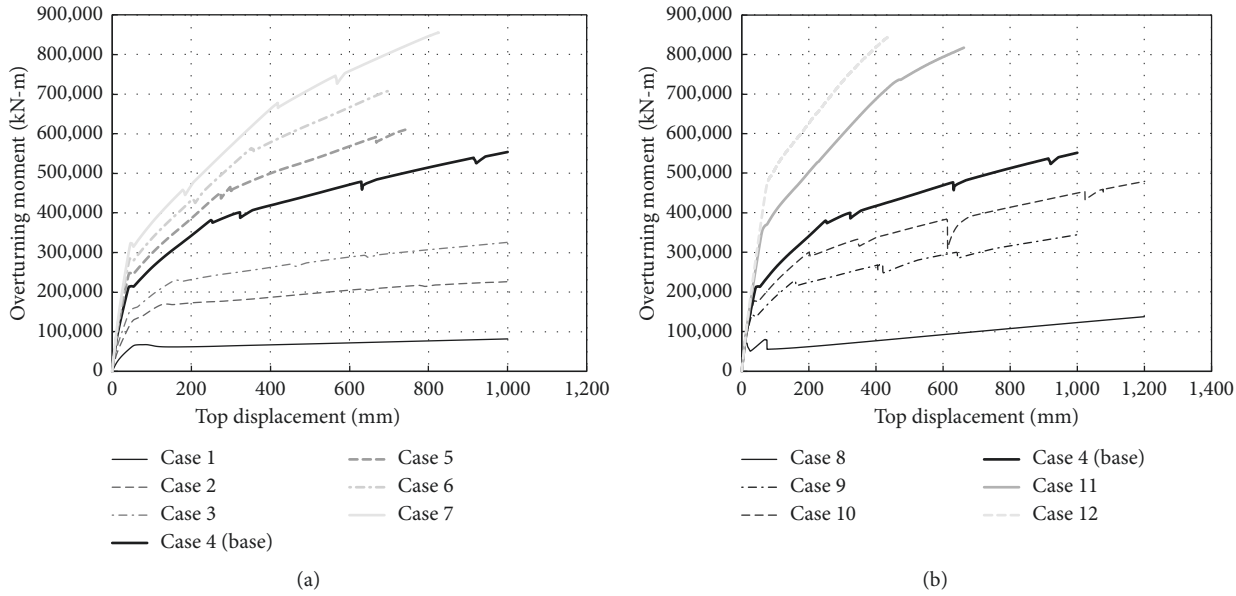

Figure 10: Parametric analysis results along with restraining abutments. (a) Variation in sectional area. (b) Variation in reinforcement steel.

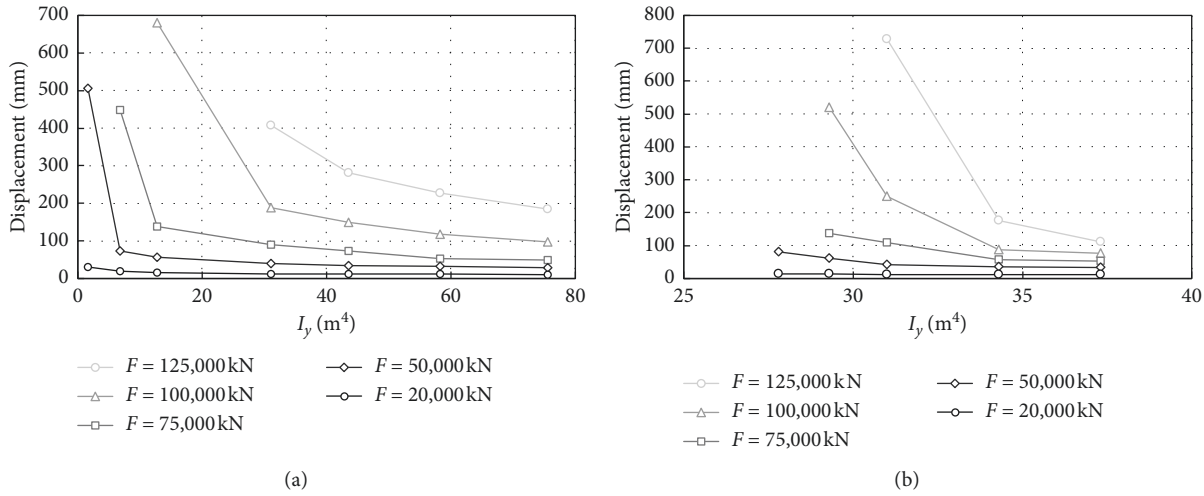

Figure 11: Analysis results for longitudinal displacements of substructure members. (a) Variation in sectional area. (b) Variation in reinforcement steel.

end-restraining abutments. Due to the innate integral characteristic of the bridge prototype at abutments, an increasing slope was still observed in the force-displacement curve of the entire frame even after the yielding of the piers. In fact, 80% of the total base shear force was distributed to the abutments while the remaining 20% was sustained by the piers.

(2) The seismic performance of the bridge prototype satisfied the performance criteria specified in Caltrans with a large margin. Consequently, the displacement ductility capacity of the entire bridge frame, $\mu_c = 6.54$, passed the specified minimum requirement of 3.0. This ensured a dependable rotational capacity in the plastic hinge regions of the bridge system.

(3) The appropriate abutment stiffness converges to a certain level to control the displacement and/or the member force capacity. When the end-restraining abutment has sufficient stiffness, any further increase in the stiffness of the end-restraining abutments yields an insignificant change in the bridge responses. Since the sectional member forces at the intermediate piers are well controlled, the end-restraining effect was also verified.

In the future, it is recommended to perform a comprehensive study for a variety of design parameters of the

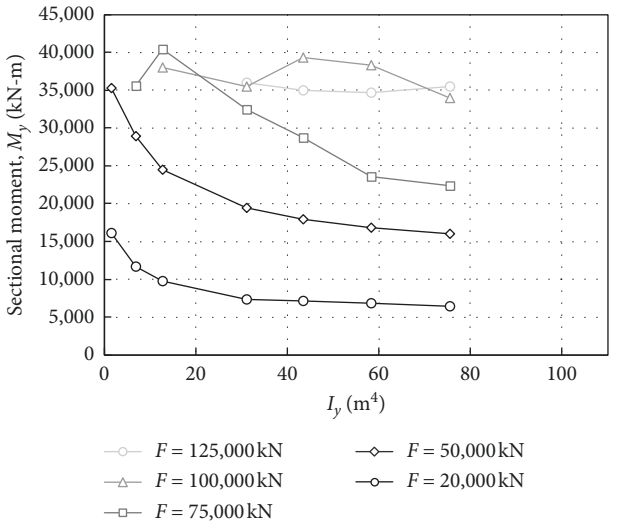

Figure 12: Sectional moment, M_y, of the substructure member (pier 3) along with abutment stiffness.

fully integral bridge using a dynamic analysis procedure. In addition, experimental verification tests are required on the details of the connected parts that make the superstructure and substructure well integrated.

Data Availability

All the data supporting the key findings of this paper are presented in the figures and tables of the article. Request for other data will be considered by the corresponding author.

Conflicts of Interest

The authors declare that they have no conflicts of interest.

Acknowledgments

The work presented in this paper was supported by the Korea Agency for Infrastructure Technology Advancement (18CTAP-C129912-02).

References

[1] S. Faraji, J. M. Ting, D. S. Crovo, and H. Ernst, "Nonlinear analysis of integral bridges: finite-element model," *Journal of Geotechnical and Geoenvironmental Engineering*, vol. 127, no. 5, pp. 454–461, 2001.

[2] L. F. Greimann, P. S. Yang, and A. M. Wolde-Tinsae, "Nonlinear analysis of integral abutment bridges," *Journal of Structural Engineering*, vol. 112, no. 10, pp. 2263–2280, 1986.

[3] B. Briseghella and T. Zordan, "An innovative steel-concrete joint for integral abutment bridges," *Journal of Traffic and Transportation Engineering (English Edition)*, vol. 2, no. 4, pp. 209–222, 2015.

[4] M. Arockiasamy, N. Butrieng, and M. Sivakumar, "State-of-the-Art of integral abutment bridges: design and practice," *Journal of Bridge Engineering*, vol. 9, no. 5, pp. 497–506, 2004.

[5] Masrilayanti, *The Behaviour of Integral Bridges under Vertical and Horizontal Earthquake Ground Motion*, PhD thesis, School of Science, Computing and Engineering University of Salford, UK, 2003.

[6] M. Prţulj, "Present condition and development of bridges-integral bridges," in *Proceedings of the 5th Slovenian Congress on Road and Traffic*, Bled, Slovenia, October 2000.

[7] G. England, N. Tsang, and D. Bush, *Integral Bridges*, Thomas Telford L.T.D. London, 2000.

[8] S. Engelsmann, J. Schlaich, and K. Schacher, *Integral Concrete Bridges*, Beton und Stahlbeton, Berlin, Germany, 1999.

[9] G. Russo, O. Bergamo, and L. Damiani, "Retrofitting a short span bridge with a semi-integral abutment bridge: the treviso bridge," *Structural Engineering International*, vol. 19, no. 2, pp. 137–141, 2009.

[10] J. Xue, *Retrofit of Existing Bridges with Concept of Integral Abutment Bridge: Static and Dynamic Parametric Analysis*, Doctoral dissertation, University of Trento, Italy, 2013.

[11] A. M. Avossa, D. Di Giacinto, P. Malangone, and F. Rizzo, "Seismic retrofit of a multispan prestressed concrete girder bridge with friction pendulum devices," *Shock and Vibration*, vol. 2018, Article ID 5679480, 22 pages, 2018.

[12] A. M. Avossa and P. Malangone, "Seismic retrofit of a pre-stressed concrete road bridge," *Ingegneria Sismica-International Journal of Earthquake Engineering*, vol. 4, pp. 5–15, 2012.

[13] D. Mitchell, R. Sexsmith, and R. Tinawi, "Seismic retrofitting techniques for bridges - a state-of-the-art report," *Canadian Journal of Civil Engineering*, vol. 21, no. 5, pp. 823–835, 1994.

[14] D. L. Kozak, J. M. LaFave, and L. A. Fahnestock, "Seismic modeling of integral abutment bridges in Illinois," *Engineering Structures*, vol. 165, no. 15, pp. 170–183, 2014.

[15] A. Paraschos and A. M. Amde, "A survey on the status of use, problems, and costs associated with integral abutment bridges," *Better Roads*, pp. 1–20, 2011.

[16] H. White, *Integral Abutment Bridges: Comparison of Current Practice between European Countries and the United States of America*, New York State Department of Transportation, New York, NY, USA, 2007.

[17] N. E. Far, S. Maleki, and M. Barghian, "Design of integral abutment bridges for combined thermal and seismic loads," *Earthquakes and Structures*, vol. 9, no. 2, pp. 415–430, 2015.

[18] M. R. Falamarz-Sheikhabadi and A. Zerva, "Effect of numerical soil-foundation-structure modeling on the seismic response of a tall bridge pier via pushover analysis," *Soil Dynamics and Earthquake Engineering*, vol. 90, no. 1, pp. 52–73, 2016.

[19] S. Erhan and M. Dicleli, "Comparative assessment of the seismic performance of integral and conventional bridges with respect to the differences at the abutments," *Bulletin of Earthquake Engineering*, vol. 13, no. 2, pp. 653–677, 2014.

[20] B. Kong, C. S. Cai, and Y. Zhang, "Parametric study of an integral abutment bridge supported by prestressed precast concrete piles," *Engineering Structures*, vol. 120, no. 1, pp. 37–48, 2016.

[21] B. Choi, J. Kwak, T. Kim, and C. Lim, "Load distribution characteristics and construction stage analysis of a fully integral railroad bridge with end-restraining abutment," *Journal of the Korean Society of Hazard Mitigation*, vol. 18, no. 2, pp. 261–270, 2018.

[22] T. Zordan, B. Briseghella, and C. Lan, "Parametric and pushover analyses on integral abutment bridge," *Engineering Structures*, vol. 33, no. 2, pp. 502–515, 2011.

[23] Caltrans, *Caltrans Seismic Design Criteria, Version 1.6*, California Department of Transportation, CA, USA, 2013.

[24] American Association of State Highway and Transportation Officials, *AASHTO Load and Resistance Factor Design (LRFD) Specifications*, Washington, DC, USA, 2010.
[25] Korean Construction Standards Center, "Guidelines for bridge seismic design standard (LSD): KDS 24 17 11," Korea, 2016.
[26] M. J. N. Priestly, F. Seible, and G. M. Calvi, *Seismic Design and Retrofit of Bridges*, Wiley, New York, NY, USA, 1974.
[27] Korean National Railroad Agency, *Korean Railway Bridge Specification*, Korea, 2016.
[28] S. Mazzoni, F. McKenna, M. H. Scott, and G. L. Fenves, *OpenSees Command Language Manual, Pacific Earthquake Engineering Research Center*, University of California, Berkeley, USA, 2007.
[29] A. S. Elnashaiand and L. Di Sarno, *Fundamentals of Earthquake Engineering*, Wiley and Sons, UK, 2008.
[30] J. B. Mander, M. J. N. Priestley, and R. Park, "Theoretical stress-strain model for confined concrete," *Journal of Structural Engineering*, vol. 114, no. 8, pp. 1804–1826, 1988.
[31] N. K. Attarchian, A. Kalantari, and A. S. Moghaddam, "Cyclic behavior modeling of rectangular RC bridge piers using OpenSees," in *Proceedings of the 4th International Conference on Computational Methods in Structural Dynamics and Earthquake Engineering*, pp. 2286–2295, Kos Island, Greece, June 2014.
[32] T.-H. Lee and D.-D. Nguyen, "Seismic vulnerability assessment of a continuous steel box girder bridge considering influence of LRB properties," *Sadhana*, vol. 43, no. 1, p. 14, 2018.
[33] D.-D. Nguyen and T.-H. Lee, "Seismic fragility curves of bridge piers accounting for ground motions in Korea," *IOP Conference Series: Earth and Environmental Science*, vol. 143, no. 1, article 012029, 2018.
[34] D. C. Kent and R. Park, "Flexural members with confined concrete," *ASCE Journal of the Structural Division*, vol. 97, no. 7, pp. 1969–1990, 1971.
[35] M. Menegotto and P. E. Pinto, "Method of analysis for cyclically loaded reinforced concrete plane frames including changes in geometry and non-elastic behavior of elements under combined normal force and bending," in *Proceedings of the IABSE Symposium of Resistance and Ultimate Deformability of Structures Acted on by Well-Defined Repeated Loads*, Lisbon, Portugal, 1973.
[36] M. G. Durante, L. Di Sarno, G. Mylonakis, C. A. Taylor, and A. L. Simonelli, "Soil-pile-structure interaction: experimental outcomes from shaking table tests," *Earthquake Engineering & Structural Dynamics*, vol. 45, no. 7, pp. 1041–1061, 2016.
[37] L. Di Sarno, F. da Porto, G. Guerrini, P. M. Calvi, G. Camata, and A. Prota, "Seismic performance of bridges during the 2016 Central Italy earthquakes," *Bulletin of Earthquake Engineering*, vol. 1–33, 2018.
[38] L. C. Reese, W. R. Cox, and F. D. Koop, "Analysis of laterally loaded piles in sand," in *Proceedings of the Offshore Technology Conference*, Houston, TX, USA, 1974.
[39] American Petroleum Institute (API), *Recommended Practice for Planning, Designing, and Construction Fixed Offshore Platforms-Working Stress Design*, Washington, DC, USA, 21st edition, 2002.